

Selective Analysis of the Elemental Composition of InGaAs/GaAs Nanoclusters by Secondary Ion Mass Spectrometry

M. N. Drozdov*, V. M. Danil'tsev, Yu. N. Drozdov, O. I. Khrykin, and P. A. Yunin

Institute for Physics of Microstructures, Russian Academy of Sciences, Nizhny Novgorod, 603950 Russia

*e-mail: drm@ipm.sci-nnov.ru

Received December 23, 2016

Abstract—New possibilities of the method of secondary ion mass spectrometry (SIMS) in application to quantitative analysis of the atomic composition of InGaAs nanoclusters in GaAs matrix are considered. Using $\text{In}_x\text{Ga}_{1-x}\text{As}$ test structures, nonlinear calibration dependences of the yield of secondary In_2As and InAs ions on the concentration of indium have been determined, which do not involve normalization to the matrix elements (Ga or As) and make possible selective analysis of the composition of nanoclusters. Using these relations, quantitative depth profiles of indium concentration were measured and statistical characteristics of the arrays of nanoclusters in InGaAs/GaAs heterostructures were determined.

DOI: 10.1134/S1063785017050170

The possibilities of using secondary ion mass spectrometry (SIMS) for the quantitative analysis of three-dimensional nanostructures are limited by the diameter of probing ion beams used in the instruments. In commercial systems such as TOF.SIMS-5 and Cameca IMS 7f, which are specially designed for high-resolution depth profiling analysis, the probing-ion-beam diameter exceeds several microns. For this reason, these instruments turn out to be poorly informative in the analysis of materials with nanoclusters and only provide data averaged over the structure. In recent works [1–3], we studied a system of $\text{Ge}_x\text{Si}_{1-x}$ nanoislands in Si matrix and discovered a new possibility of determining germanium concentration in these nanoislands by SIMS based on a nonlinear relationship between the yield of secondary ions and the concentration of germanium. The nonlinear calibration dependence was constructed for the ratio of negative secondary ions Ge_2/Ge versus Ge concentration in the entire range of $0 < x < 1$, which did not involve normalization to secondary Si ions of the matrix. Since both secondary ions of Ge_2 and Ge were only emitted from GeSi nanoislands, calibration for the Ge_2/Ge ratio allowed the concentration of Ge in these clusters to be selectively determined without averaging over the silicon matrix. Nonlinear matrix effects in SIMS usually strongly complicate the quantitative analysis of multicomponent structures and require finding linear calibration relations between the secondary ion yield and analyte content by analogy with the method of relative sensitivity factors in the analysis of atomic-impurity concentration [4]. In contrast, in the proposed approach [2, 3], the possibility of analy-

sis is based on the strong manifestation of matrix effects leading to nonlinear calibration relations.

It should be noted that analogous approach has been later used by Franquet et al. [5, 6] for the analysis of GeSi and A_3B_5 nanoclusters formed in Si_3N_4 and SiO_2 matrices by electron-beam lithography techniques. This approach is alternatively called “self-focusing SIMS” [5, 6], but we believe that the term “self-focusing” is not quite appropriate in this case, because this method characterizes the properties of an array of nanoobjects rather than selecting and probing one of these nanoobjects. The primary ion beam is not modified (what is usually implied by “self-focusing”), but only a certain component of the total secondary ion yield is selectively separated and analyzed. We consider that the term “selective” better characterizes the SIMS concept under consideration. In [5], analysis of Ge/Si nanoobjects in passivating $\text{Si}_3\text{N}_4/\text{SiO}_2$ matrix was based on Ge_2/GeSi calibration (analogous to that used in our works [2, 3]), while A_3B_5 nanoparticles in SiO_2 matrix [6] represented a simpler system with the matrix not containing elements of the nanoobjects studied, which allowed a simple variant of calibrating the In and Al atomic concentration in GaAs to be used. However, it is still not completely clear whether this selective analysis by SIMS is always possible for A_3B_5 systems—in particular, whether nonlinear calibration dependences (analogous to those for Ge_2/Ge) can be used.

In the present work, the approach of selective SIMS has been developed for analysis of an array of InGaAs quantum dots in GaAs matrix. New nonlinear calibration relations for various types of secondary

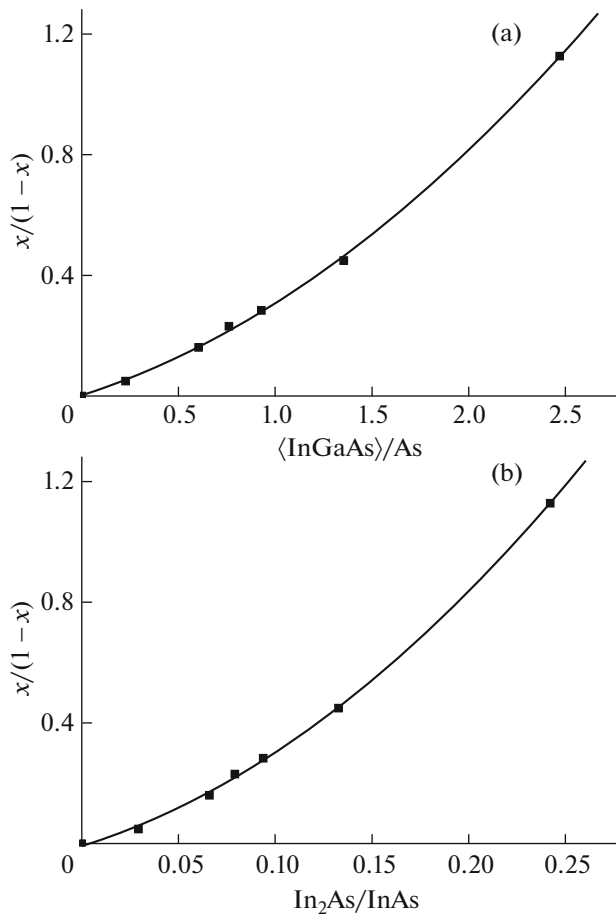


Fig. 1. Calibration curves of $x/(1-x)$ versus relative yields of secondary ions: (a) $\langle \text{InGaAs} \rangle / \text{As}$ obtained for $\text{In}_x\text{Ga}_{1-x}\text{As}$ test structures with different compositions; (b) $\text{In}_2\text{As} / \text{InAs}$. Points represent experimental data, solid curves show approximations by (a) formula (1) and (b) formula (2).

ions containing indium and only related to the quantum dots have been obtained. On this basis, quantitative analysis of indium concentration was performed and statistical characteristics of quantum-dot arrays in related heterostructures were determined.

The SIMS measurements have been performed on a TOF.SIMS-5 instrument equipped with a time-of-flight (TOF) mass analyzer and two ion guns performing different functions—sputtering and probing, both operating in a pulsed mode. The sputtering was carried out using 1-keV cesium ions, while the probing was performed using 25-keV bismuth ions. The use of Bi_3^+ cluster ions provided a higher yield of secondary ions with greater masses as compared to the case of monatomic Bi^+ ions. The probing ion beam was scanned over an area of 128×128 pixels, from which negative secondary ions of As, InAs, $\text{In}^{69}\text{GaAs}$, $\text{In}^{71}\text{GaAs}$, and In_2As were detected.

Calibration relations were determined using two specially grown test heterostructures with $\text{In}_x\text{Ga}_{1-x}\text{As}$ layers on GaAs substrates. The structures had different stepped profiles of indium concentration (x): 0.047–0.130–0.221 in the first case and 0.188–0.31 in the second case. In addition, we have studied a heterostructure with an $\text{In}_{0.53}\text{Ga}_{0.47}\text{As}$ layer on an InP substrate. The concentration of indium in each layer was determined by X-ray diffraction. The obtained calibration relations were used to study two sample structures with InGaAs quantum-dot arrays. In structure #A, the quantum dots were grown on the GaAs surface, while the quantum dots were overgrown by a thin layer of GaAs in structure #B. All heterostructures were grown by metalorganic vapor-phase epitaxy. More detailed information on the growth and optical properties of these structures was reported previously [7–9].

Figure 1 shows calibration curves of the relative yield of secondary ions versus relative content of indium, which were obtained using the test structures. From among the possible variants, the simplest relations were selected that allowed indium concentration x to be determined by means of calculations. In Fig. 1a, ratio $x/(1-x)$ is plotted versus relative yield of ions $\langle \text{InGaAs} \rangle / \text{As}$, where $\langle \text{InGaAs} \rangle$ is the sum of several secondary cluster ions:

$$\langle \text{InGaAs} \rangle = \text{InAs} + \text{In}^{69}\text{GaAs} + \text{In}^{71}\text{GaAs}.$$

The experimental curve in Fig. 1a can be approximated by the following quadratic dependence:

$$\begin{aligned} x/(1-x) = & 0.205\langle \text{InGaAs} \rangle / \text{As} \\ & + 0.101(\langle \text{InGaAs} \rangle / \text{As})^2. \end{aligned} \quad (1)$$

Figure 1b shows the plot of the ratio $x/(1-x)$ versus relative yield of secondary ions $\text{In}_2\text{As} / \text{InAs}$, which can also be approximated by a quadratic dependence as follows:

$$\begin{aligned} x/(1-x) = & 1.98(\text{In}_2\text{As} / \text{InAs}) \\ & + 11.22(\text{In}_2\text{As} / \text{InAs})^2. \end{aligned} \quad (2)$$

The correlation coefficient between experimental data and expressions (1) and (2) is $R \sim 0.9994$, which is indicative of a high accuracy of these approximations.

Expression (1) is analogous to the linear calibration dependence for GeSi [1–3] and involves normalization to the matrix element As. Expression (2) employs the normalization of secondary In_2As ions to InAs ions and is analogous to the nonlinear calibration dependence for Ge_2/Ge [1–3]. For the system of quantum dots InGaAs/GaAs, this calibration involves only the secondary ions emitted from quantum dots. At the same time, secondary As ions taken into account in expression (1) are emitted both from quantum dots and the surrounding GaAs matrix.

Another possible regime for SIMS analysis of InGaAs quantum dots is based on the use of As, In, and In₂ secondary ions during the sputtering by oxygen ions. In this case, In₂/In calibration is analogous to that described by formula (2). These calibration relations were also obtained, but it turned out that large concentration of indium in quantum dots led to very high yield of positive secondary ions of ¹¹³In and ¹¹⁵In isotopes such that the detector of TOF.SIMS-5 mass analyzer was in the regime of signal saturation, which significantly distorted the results of quantitative analysis. This problem could not be solved by correction for the dead time of detector used in the TOF.SIMS-5 instrument. The most widely used regime of quantitative SIMS analysis of the elemental composition of InGaAs-based heterostructures employs the detection of secondary cluster ions of CsIn, CsGa, and CsAs during the sputtering with cesium ions, which is known as the “CsM⁺ approach.” However, this regime only admits using a linear calibration relation analogous to formula (1).

For test heterostructures with In_{0.18}Ga_{0.82}As quantum well, calibration relations (1) and (2) give close depth profiles of indium concentration x , which only differ in the dynamic range of x variation. This result confirms the correctness of this calibration for planar structures under consideration. Figure 2 shows the depth profiles of indium concentration x in structure #A with quantum dots on the substrate surface, where curves 1 and 2 are plotted using calibration relations (1) and (2), respectively. As can be seen, the concentration of indium in quantum dots according to formula (2) (curve 2) amounts to 0.8 and is significantly (about six times) greater than the value of 0.14 given by formula (1) (curve 1). The reason for this discrepancy is quite clear in view of the above considerations. Indeed, curve 1 gives an x value averaged over the entire region of analysis, while curve 2 gives x immediately in quantum dots. The two curves differ not only by their maximum x values, but also by the character of x variation with the depth: curve 1 rapidly decays with the depth and its width at half maximum corresponds to the height of quantum dots (~10–12 nm), whereas curve 2 decreases much more slowly. This distinction is also related to the difference of calibration relations. Indeed, during the ion-beam sputtering of the array of quantum dots, the average x value decreases in proportion to their relative area on the sample surface. At the same time the indium concentration x in quantum dots remains almost unchanged and, hence, curve 2 decays very slowly. At depths above 25–30 nm, the error of curve 2 increases as a result of decreasing yields of secondary In₂As and InAs ions entering into the numerator and denominator of expression (2). An additional uncertainty is introduced by the artifacts of ion sputtering such as preferential sputtering and atomic mixing.

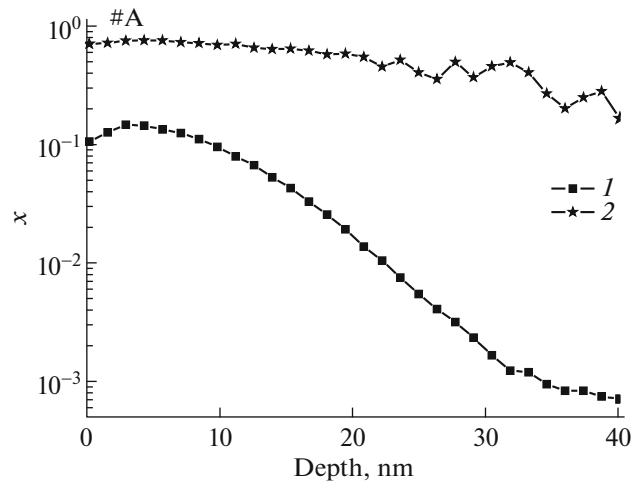


Fig. 2. Depth profiles of indium concentration x in structure #A with quantum dots on the substrate surface. Curves 1 and 2 are obtained using calibration relations (1) and (2), respectively.

It should also be noted that calibration relation (2) was obtained in the interval of indium concentrations from 0 to 0.53, while the value $x \sim 0.8$ in quantum dots is above this interval. Nevertheless, we believe that the error of relation (2) in the interval of $0.53 < x < 1$ is also small and does not exceed several atomic percent. In particular, an experiment for pure InAs ($x = 1$) showed that formula (2) slightly understated real indium concentration and yielded $x = 0.96$.

Using the data of depth profiling retained in each pixel of the area scanned by the probing ion beam in a TOF-SIMS-5 instrument, it is possible to reconstruct a lateral image of the region of analysis in secondary ions and construct the corresponding map of x distribution over the surface [3]. We have performed this processing for structures #A and #B. Figure 3a shows histograms of the indium concentration distribution over pixels in the area scanned by the probing ion beam in structure #A, obtained using “linear” (curve 1) and “nonlinear” (curve 2) calibration relations (1) and (2), respectively. Curve 2 shows statistical characteristics of the array, such as the average indium concentration in quantum dots and the width of this distribution. For example, the distribution width for structure #A is about 30 at %. The histograms were obtained for the entire array of quantum dots. If necessary, these histograms can be constructed for two sections in transverse directions so as to study asymmetry of the array. Figure 3b shows the analogous results for structure #B, in which the quantum-dot array was overgrown by a thin GaAs layer. Here, curve 2 shows that the average indium concentration in quantum dots of structure #B amounts to ~0.4. Note that SIMS analysis using calibration (1) provides a lower indium concentration in quantum dots of structure #B, with a maximum value of $x \sim 0.11$ (Fig. 3b, curve 1).

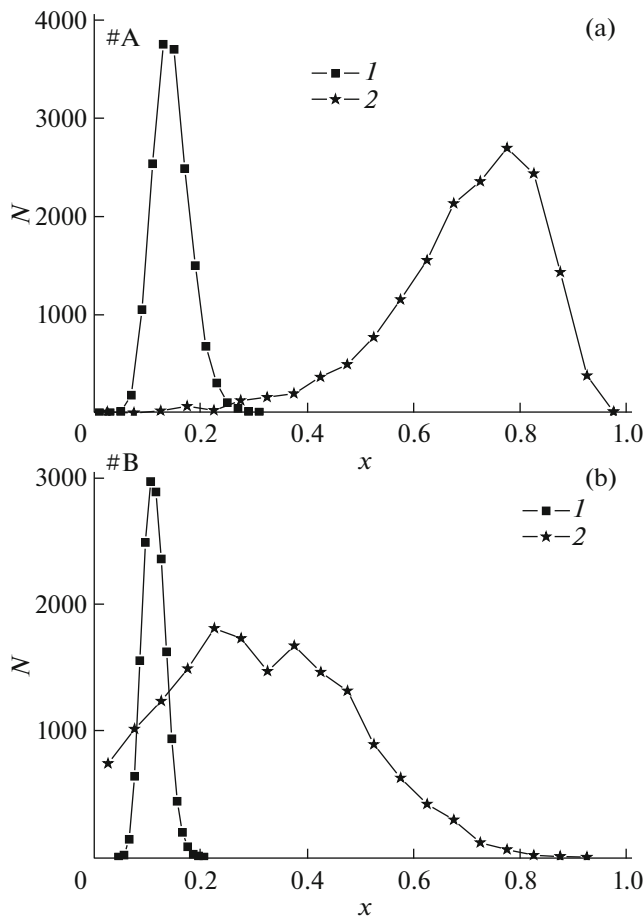


Fig. 3. Histograms of the distribution of indium concentration x with respect to number N of pixels in the area scanned by the probing ion beam in (a) structure #A and (b) structure #B. Curves 1 and 2 are obtained using calibration relations (1) and (2), respectively.

Thus, we have obtained new quantitative calibration relations for indium concentration in the $\text{In}_x\text{Ga}_{1-x}\text{As}$ system, which allow the characteristics of InGaAs quantum dots in GaAs matrix to be studied using standard SIMS equipment with broad probing ion beams (with a beam diameter much greater than the quantum-dot size). By analogy with analysis of the GeSi system using Ge_2/Ge calibration, the $\text{In}_2\text{As}/\text{InAs}$ ratio for InGaAs structures exhibits a monotonic concentration dependence that makes possible the selective quantitative SIMS analysis of structures with nanoclusters. This result suggests a universal character of the method of selective analysis of nanoobjects in a matrix during depth profiling, making it quantitative due to proper choice of detected cluster ions. On the other hand, this is indicative of a strong manifestation of nonlinear matrix effects in the InGaAs system.

The proposed approach does not require any additional information about the heterostructures being studied. By depth profiling with the use of various secondary ions, it is possible to distinguish planar and

three-dimensional structures, determine average indium concentration in quantum dots, and determine their characteristic height. Based on these measurements, it is possible to study the lateral distribution of indium concentration on the surface and determine the statistical characteristics of quantum-dot arrays by constructing a histogram of indium concentration distribution over pixels in the area scanned by the probing ion beam and estimating its width and asymmetry in transverse directions. These characteristics have been determined for InGaAs quantum-dot arrays, both exposed on the surface and overgrown by a thin GaAs layer. Independent verification of the obtained data was provided by their comparison to the results of analysis of the quantum-dot array on the surface of structure #A by different methods. Atomic-force-microscopy measurement of the heights of quantum dots gave an average value of about 10 nm, and the indium concentration estimated from X-ray diffraction measurements amounted to 0.9 ± 0.05 . These values are close to the results obtained by the proposed selective SIMS method.

Acknowledgments. This work was performed using instrumentation of the Collective Equipment Share Center at the Institute for Physics of Microstructures (Nizhny Novgorod) and supported in part by the Russian Foundation for Basic Research, project no. 15-02-02947.

REFERENCES

1. M. N. Drozdov, Yu. N. Drozdov, A. V. Novikov, P. A. Yunin, and D. V. Yurasov, *Semiconductors* **48**, 1109 (2014).
2. M. N. Drozdov, Yu. N. Drozdov, N. D. Zakharov, D. N. Lobanov, A. V. Novikov, P. A. Yunin, and D. V. Yurasov, *Tech. Phys. Lett.* **40**, 601 (2014).
3. M. N. Drozdov, Yu. N. Drozdov, A. V. Novikov, P. A. Yunin, and D. V. Yurasov, *Tech. Phys. Lett.* **42**, 243 (2016).
4. R. G. Wilson, *Int. J. Mass Spectrom. Ion Processes* **143**, 43 (1995).
5. A. Franquet, B. Douhard, D. Melkonyan, et al., *Appl. Surf. Sci.* **365**, 143 (2016).
6. A. Franquet, B. Douhard, T. Conard, et al., *J. Vac. Sci. Technol. B* **34**, 03H127-1 (2016).
7. V. I. Shashkin, V. M. Danil'tsev, M. N. Drozdov, et al., *Prikl. Fiz.*, No. 2, 73 (2007).
8. M. N. Drozdov, V. M. Danil'tsev, L. D. Moldavskaya, and V. I. Shashkin, *Tech. Phys. Lett.* **34**, 1 (2008).
9. M. N. Drozdov, N. V. Vostokov, V. M. Danil'tsev, Yu. N. Drozdov, L. D. Moldavskaya, A. V. Murel, and V. I. Shashkin, *Semiconductors* **42**, 298 (2008).

Translated by P. Pozdeev